



Cite this: *Dalton Trans.*, 2024, **53**, 17157

Received 1st October 2024,
Accepted 9th October 2024

DOI: 10.1039/d4dt02767a

rsc.li/dalton

Not so inert *mer*-tris-chelate cobalt(III) complex of a hydroxy-pyridine functionalized NHC ligand for cyclic carbonate synthesis†‡

Rhitwika Chowdhury, Irshad Ahmad Bhat,§ Sharad Kumar Sachan and Ganapathi Anantharaman *

The homoleptic hydroxy-pyridine functionalized Co(III)–NHC complex (2) demonstrates extraordinary catalytic activity towards the CO₂ cycloaddition under mild conditions. Using this catalyst and TBAB, the highest TON (666 667) and TOF (52 713 h^{−1}) were achieved compared to previously reported cobalt catalysts.

The industrial revolution and the ensuing excessive usage of fossil fuels have resulted in immoderate amounts of carbon dioxide (CO₂), a key ingredient in greenhouse gases and believed to be liable for climate change. Since the start of the industrial age, the amount of CO₂ in the Earth's atmosphere has increased by 50%, reaching almost 427 ppm by June 2024.^{1,2} Although carbon capture and storage (CCS) is one of the finest methods, like adsorption-based sequestration or mitigation of CO₂, converting carbon dioxide (CCUS) to value-added products is more beneficial. CO₂ is a cheap, sustainable, non-toxic, and abundant C1 source.^{1,2} A variety of (in)organic compounds employing CO₂ as a starting material have been prepared in recent decades, including the synthesis of urea, esters, methane, methanol, salicylic acid, cyclic organic carbonates (COCs), polycarbonates (PCs) and inorganic carbonates.³ In particular, COC is a valuable heterocyclic precursor that has been extensively utilized as a polar aprotic solvent, battery electrolyte, and monomer for producing PC and as an intermediate for producing fine chemicals.^{4–6} Thus, synthesizing COC by adding CO₂ to epoxides is a 100% atom-economical process for CO₂ fixation. However, CO₂ conversion is difficult under mild conditions because of its thermodynamic stability and kinetic inertness. A catalyst that can reduce this

reasonably large amount of free energy is commonly employed to overcome these obstacles. Multiple catalysts, based on either heterogeneous systems, including metal oxides, organo-catalysts, ion-exchange resins, and metal-organic frameworks (MOFs), or homogeneous metal complexes, like ionic liquids, multiple salen, salophen, and porphyrin ligands, have been successfully created during the past few decades to catalyse the cycloaddition reaction.^{7–11} Among them, cobalt complexes were more effective for cyclic carbonate synthesis. Verpoort and co-workers reported dinuclear cobalt or Co(III)–ONO pincer complexes as catalysts with TOF values of 3333 h^{−1} and 4166 h^{−1}, respectively (Chart 1).¹²

Octahedral tris-chelate complexes of transition metal ions have been known for over a century, and their geometrical structures, namely facial (*fac*) and meridional (*mer*) and their optical forms, are widely explored. Among them, the *d*⁶ metal complexes are substitutionally inert under normal ambient conditions; hence, their utility as catalysts is seldom explored and reported in the literature.¹³ In contrast to the simple bidentate donor moieties, multifunctional NHC ligands containing hard/intermediate donor groups are beneficial for developing robust catalysts due to the chelate effect. Moreover, the additional donor moiety will exhibit hemilability or bifunctional properties that may be useful in generating a vacant coordination site during catalysis. Keeping this in view, the electronic/steric influence leading to the robustness of NHC–metal complexes and their utility in homogeneous catalysis has continued to be one of the pertinent topics in metal–NHC chemistry over the past three decades.^{13–15} Various research groups have demonstrated the implications of hemilabile

Department of Chemistry, Indian Institute of Technology Kanpur (IITK), Kanpur-208016, Uttar Pradesh, India. E-mail: garaman@iitk.ac.in

† Dedicated to Professor Vinod K. Singh on the occasion of his 65th Birthday.

‡ Electronic supplementary information (ESI) available: Experimental details, structural characterization of 2 including X-ray diffraction studies, as well as NMR data and comparison table of COCs. CCDC 2368776. For ESI and crystallographic data in CIF or other electronic format see DOI: <https://doi.org/10.1039/d4dt02767a>

§ Current address: Department of Chemistry, Amar Singh College, Cluster University Srinagar, Jammu and Kashmir-190008, India.

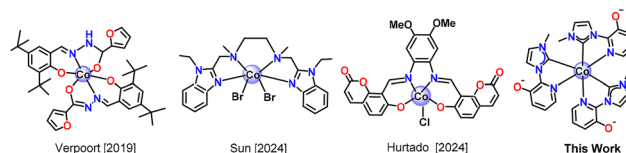


Chart 1 Representative cobalt catalysts for COC preparation.

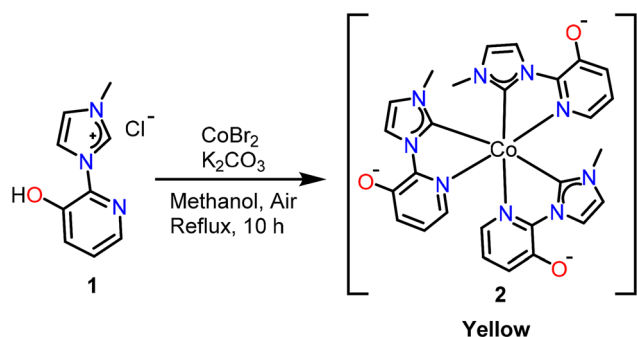
ligands in numerous organic transformations. We have recently investigated the square planar bis-chelate complexes of nickel(II) and copper(II) using hydroxypyridine functionalized imidazol-2-ylidenes and evaluated them as catalysts for the Kumada–Tamao–Corriu (KTC) cross-coupling and aerobic oxidation of alcohol reactions. Intrigued by the diversity in the chelation of the hydroxypyridine functionalized imidazole-2-ylidene (IMepyO) ligand coordination to metal ions, like binding through normal/abnormal carbene using pyridinoxy N/O-centres to the metal ion, this study was extended to the synthesis of octahedral metal complexes using cobalt ions. Moreover, the hemilability of these ligands and the metallo-base character of $M(II)$ -NHC [$M = Ni, Cu$] complexes were exemplified during the earlier reported catalytic studies, which prompted us to utilize the $Co(III)$ -NHC complex for the cycloaddition reaction with environmentally noxious CO_2 gas and epoxides.¹⁶ Although various $Co(III)$ complexes are widely employed for COC preparation, the $Co(III)$ -NHC complexes are rarely employed as catalysts.¹⁷ Herein, we report the synthesis, structural characterization, and catalytic activity with the highest TOF ($52\,713\,h^{-1}$) of the unique *mer*- $Co(\kappa CN-IMepyO)_3$ complex. Also, to the best of our knowledge, this was the highest TOF ever obtained employing binary catalysts of cobalt complexes with TBAB with epichlorohydrin (ECH) as a substrate.

The reactions of $CoBr_2$ with hydroxypyridine functionalized imidazolium salt **1** in air afforded the tris-chelate complex $[Co(\kappa CN-IMepyO)_3]$ (**2**) as a yellow crystalline material in moderate yield (Scheme 1).¹⁸ The air stability of **2** prompted complete characterization by spectroscopic, spectrometric, elemental, and single-crystal X-ray diffraction analyses (Fig. S1–S3 and Tables S1–S3†). The appearance of sharp signals in the NMR spectrum indicates that the $Co(II)$ precursor is oxidized to $Co(III)$ under the reaction conditions. The disappearance of the C2-H imidazolium proton and the appearance of other proton peaks, such as N-Me, imidazol-2-ylidene, and pyridyl protons, in the shielded and deshielded regions, respectively, are indicative of the formation of the Co -IMepyO complex. Notably, the peak for Im-4H appears at 5.66 ppm ($DMSO-d_6$)/6.06 ppm (CD_3OD), suggesting the formation of $C\equiv N$ wherein the zwitterionic 'O' interacts with Im-4H. Furthermore, the

elemental analysis and ESI-MS(+) indicate the formation of a tris-chelate complex with the formula $[Co(\kappa CN-IMepyO)_3]$ (582.1407). Single-crystal X-ray diffraction studies were used to ascertain the zwitterionic tris-chelate complex of **2** and the coordination behavior of IMepyO to the metal centre.

$2 \cdot 5.5\,H_2O$ crystallizes in a monoclinic $P2_1/n$ space group with the central $Co(III)$ ion bound by three NHC carbene carbons (abbreviated as C_{NHC}) and three N-atoms of the pyridonate in a *mer*-configuration (Fig. 1). Out of the three $Co(III)$ – C_{NHC} bond distances, the *meridional* bonds are almost similar ($Co1-C1$ av. $1.931(5)\,Å$), being *trans* to each other, but appreciably longer than the remaining one ($Co1-C10$ $1.886(5)\,Å$), which is *trans* to the N-atom of one of the pyridonate moieties. The latter $Co-C_{NHC}$ value is quite shorter than the reported values. Although these values are comparable to the known $Co-C_{NHC}$ bonds, this is one of the first *meridional* tris-chelate cobalt complexes to be reported in the literature.^{15a,b} Besides, the $Co-N$ bond distances of pyridonate fall within the range of $1.953(4)$ – $1.987(4)\,Å$, which is closer to the reported value ($1.962(4)\,Å$).¹⁹ In all the three bidentate ligands, the imidazole-2-ylidene ring is almost coplanar with the pyridonate ring with very small dihedral angles (3.46° , 3.48° , and 6.75°) between the two rings in the ligand. Furthermore, the heterobidentate ligands possess an average bite angle of around 82° , and the five-membered metallacycle formed by each ligand is planar with the metal atom within the plane of the metallacycle.

The stability of complex **2** in both solution and the solid state has prompted us to exploit it as a catalyst for the cycloaddition of CO_2 to epoxides under solvent-free conditions using ECH as a model substrate, with and without the cocatalyst tetrabutylammonium bromide (TBAB) and by varying the reaction conditions, such as temperature, CO_2 pressure, molar ratio of the substrate to catalyst, and the reaction time. In addition, the catalytic potential of the precursors utilized for the synthesis of **2**, like anhyd. $CoBr_2$ and free ligand **1**, was also investigated. Although the cyclic carbonate formation was



Scheme 1 Synthesis of **2**.

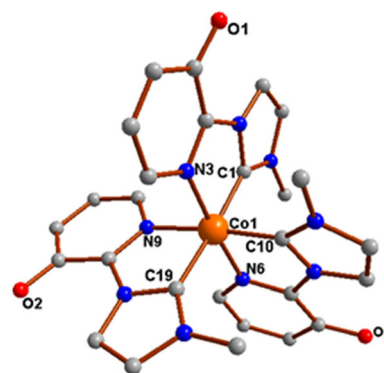


Fig. 1 Crystal structure of **2**. Hydrogen atoms and 5.5 lattice water molecules have been removed for clarity. Selected bond lengths ($Å$) and angles ($^\circ$): $Co1-C1$ $1.931(5)$; $Co1-C10$ $1.886(5)$; $Co1-C19$ $1.940(5)$; $Co1-N3$ $1.953(4)$; $Co1-N6$ $1.959(4)$; $Co1-N9$ $1.987(4)$; $C1-Co1-C19$ $175.5(2)$; $C1-Co1-C10$ $86.7(2)$, $N3-Co1-N6$ $175.99(16)$, $N9-Co1-C10$ $175.10(19)$.

observed using **2** and TBAB under neat conditions at room temperature (RT) and 1 atm. pressure, the conversion took a longer reaction time (Table 1, entries 1–4). Also, no conversion of ECH was observed at RT in the presence of CoBr₂ as a catalyst (Table 1, entry 5). Meanwhile, low to moderate conversion was observed at high temperatures when CoBr₂ or **1** was used as a catalyst in the presence of TBAB (Table 1, entries 7 and 8). These results suggest that the catalyst design and temperature significantly diminish the activation energy barrier for the cycloaddition of CO₂ to epoxide. Subsequently, the catalyst and cocatalyst concentration in the cycloaddition reaction was probed, keeping 100 °C temperature, 1 atm. pressure, and 3 h of time constant (Table 1, entries 9–15). The conversion to cyclic carbonate was highest for 0.043 mol% of the catalyst (Table 1, entry 11), whereas the conversion decreased upon lowering the loading of either the catalyst or co-catalyst (Table 1, entries 12–15). This indicates that both catalyst and cocatalyst together play an important role as a binary catalyst in the formation of cyclic carbonate. Curiously, the cycloaddition reaction proceeds without TBAB as well, by maintaining the other experimental parameters intact; however, the quantitative conversion was obtained only when the temperature was increased from 100 to 120 °C. Besides, the increase of CO₂ gas pressure in the reaction did not have an impact; instead, quantitative conversion of cyclic carbonate was achieved when the temperature was 120 °C (Table 1, entries 16–19), which once again authenticates that temperature plays

a crucial role in this reaction. In summary, the conditions used in entry 11 became the best-optimized conditions for cyclic carbonate preparation using the starting materials CO₂ and epoxide. Therefore, the substrate scope of this reaction was investigated using various terminal epoxides like aliphatic, aromatic, and ether substitutions in the side arm, as well as internal epoxides and bis-epoxide moieties, with varying times for conversion.

Terminal epoxides with varying substitutions were examined for cycloaddition reactions. For all the terminal mono-epoxides, except for styrene epoxide, the conversion of the products was exceptional, yielding the corresponding cyclic carbonates quantitatively. Similarly, the more challenging cyclohexane oxide **3f**, *i.e.*, an internal epoxide, can be converted (91%) to the corresponding *cis*^{11a,20e} cyclic carbonate **4f** in 24 h by taking twice the ratio of **2** (0.86 mol%) and TBAB (2 mol%).

In addition, the quantitative formation of bis-cyclic carbonate, starting from neopentyl glycol diglycidyl ether (NPGDGE), was observed under similar experimental conditions. Overall, in all cases, superior conversion of epoxides with >99% product selectivity using catalyst **2** (0.043 mol%) and TBAB (0.2 mol%) at 100 °C and 1 atm. pressure was achieved (Fig. 2). Moreover, the scalability of the reaction and the reusability of the catalysts for their sustainability and potential utility in the industry were studied using a large amount of ECH (Table 1, entries 20–25). The highest TON (Table 1, entry 24) and TOF (Table 1, entry 21) were achieved by varying the catalyst to co-

Table 1 Results of the cycloaddition reaction of ECH^a and CO₂

Entry	Catalysts (mol%)	Temp. (°C)	pCO ₂ (atm)	Time (h)	Conv. ^b (%)	TON ^c	TOF ^d (h ⁻¹)
1	2 (0.43)	RT	1	12	15	35	3
2	2 (0.086)	RT	1	12	21	244	20
3	2 (0.043)	RT	1	12	25	581	48
4	2 (0.0086)	RT	1	12	10	1163	97
5	CoBr ₂ (0.043)	RT	1	3	0	0	0
6	—	100	1	3	31	—	—
7	CoBr ₂ (0.043)	100	1	3	21	488	163
8	1 (0.043)	100	1	3	43	1000	333
9	2 (0.43)	100	1	3	86	200	67
10	2 (0.086)	100	1	3	87	1012	337
11	2 (0.043)	100	1	3	>99	2325	775
12	2 (0.0086)	100	1	3	88	10 232	3411
13	2 (0.0043)	100	1	3	75	17 442	5814
14	2 (0.043)	100	1	3	52	1209	403
15	2 (0.043)	100	1	3	31	721	240
16	2 (0.043)	120	1	3	>99	2325	775
17	2 (0.043)	100	10	3	25	581	194
18	2 (0.043)	120	4	3	>99	2325	775
19	2 (0.043)	100	1	3	28	651	217
20	2 (0.00086)	100	1	3	71	82 558	27 519
21	2 (0.00043)	100	1	3	68	158 139	52 713
22	2 (0.00043)	100	1	8	>99	232 558	29 070
23	2 (0.00015)	100	1	12	68	453 333	37 778
24	2 (0.00015)	100	1	24	>99	666 667	27 778
25	2 (0.00015)	100	1	24	42	280 000	11 666

^a Reaction conditions: ECH (10 mmol for entries {1–11}; 40 mmol for entries {12–19}; 400 mmol for entries 20–25). ^b Conversions based on the ¹H NMR spectrum. ^c TON: moles of the substrate converted to the product/moles of the catalyst used. ^d TOF: TON/total reaction time (h). In all reactions TBAB with 0.2 mol% was used except for entry 14, 0.02 mol%; entry 15, 0.002 mol%; and entry 25, 0.00015 mol%, whereas for the reactions in entries 16–19, no TBAB was used.

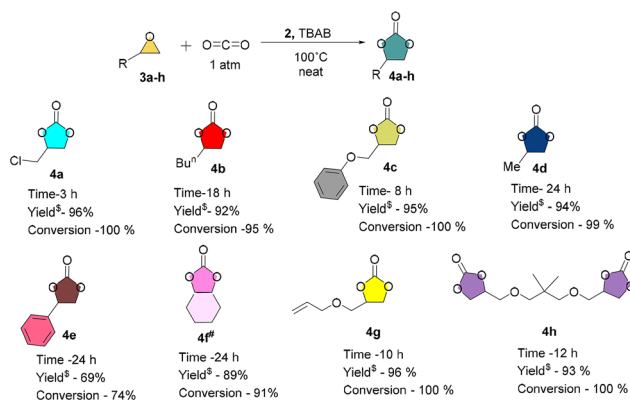
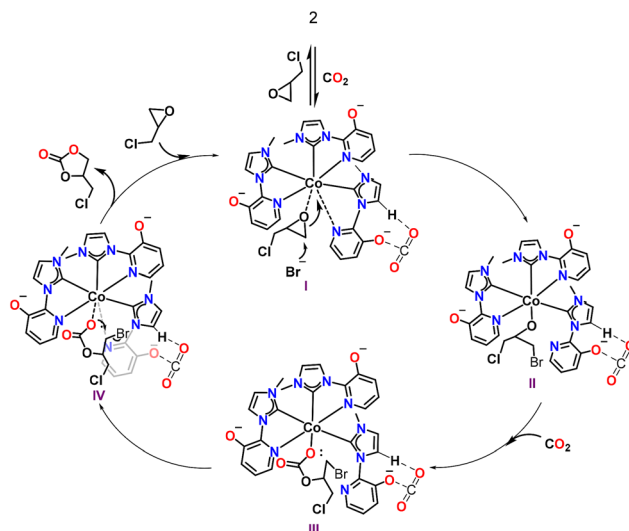


Fig. 2 Cycloaddition of epoxides with CO₂ using 2 (0.043 mol%), TBAB (0.2 mol%), #2 (0.86 mol%), TBAB (2 mol%); [§]isolated yield.

catalyst ratio as compared to the 1 : 1 ratio (Table 1, entry 25). Although a large conversion to COC was observed due to the facile ring opening of ECH, due to the presence of electron-withdrawing Cl, the exigency of the binary catalyst performance compared to other cobalt catalysts or other Earth-abundant metal catalysts under 1 atm. pressure of CO₂ (Tables S4 and S5[†]) is worthwhile to note. Furthermore, a reusability test was performed under the same optimized conditions (Table 1, entry 11), demonstrating that the catalyst can be reused without separating the catalyst at least five times and without any significant loss of catalytic activity (Fig. S28 and S29[†]).

Thermally robust metal complexes are preferred for preparing cyclic carbonate at the industrial scale. It is well known that the *d*⁶-low spin compounds are substitutionally inert at temperatures lower than 100 °C.^{3d,20} This is often observed in the CO₂ cycloaddition reaction with epoxide at RT, where the cycloaddition is slow and only a lower conversion of 3a to 4a is observed. Meanwhile, catalysis is very facile at an elevated temperature of 100 °C, and the yields of cyclic carbonates (4a–4d, 4g, and 4h) are almost quantitative in a shorter time. In addition, the reaction goes smoothly without the need for a cocatalyst. Therefore, the reaction must have proceeded by coordinating epoxide instead of one of the existing pyridine Co–N bonds. A closer look at the hemilability of the chelate ligand in 2, using variable temperature NMR measurements, and the nature of epoxide binding reveal that the ECH binds to the Lewis acidic Co³⁺ weakly, as observed in the combined ECH and 2 NMR spectra wherein ECH hydrogens (~0.07 ppm) show minor shielding in comparison with the parent ECH hydrogen atoms. However, there was no change in the corresponding pyridine or imidazole backbone hydrogen units (Fig. S21 and S22[†]). In addition, ESI-MS shows a 1 : 1 ratio of catalyst and ECH complex formation (Fig. S23[†]). Based on this information, a plausible mechanism for the conversion of epichlorohydrin to the corresponding cyclic carbonate was proposed in the presence of catalyst 2 (Scheme 2 and Scheme S1[†]) with and without the cocatalyst TBAB.^{1,9,21} The first activation occurs by coordinating epoxide oxygen with the metal center and not by CO₂ insertion (Table 1, entries 16–19). The second



Scheme 2 Proposed mechanism of cycloaddition by ECH with CO₂ using 2 and NBu₄Br. The NBu₄⁺ unit in the catalytic steps I to IV is not shown here.

step proceeds through (a) dissociation of pyridine due to the *trans* effect of the carbene carbon and (b) the epoxide ring opening, which may be supported by CO₂ binding at the *exo* position of the pyridonate oxygen ion either by the added nucleophile (Br[−]) or by an internal nucleophile, the free nitrogen lone pair of dissociated Co–Npy bonds of pyridine (Fig. S24–S27[†]). Subsequently, the insertion of CO₂ occurs between metal-alkoxide bonds, leading to metal-bound acyclic organocarbonate formation. Finally, cyclization occurs through the backbiting of oxygen to obtain the expected cyclic carbonate with the regenerated epoxide-bound catalyst.

Conclusions

In conclusion, a robust *meridional* hydroxypyridine functionalized Co(III)–NHC complex 2 was synthesized. Together with the cocatalyst, 2 exhibits high catalytic activity in the CO₂ cycloaddition process with epoxide. The cycloaddition is selective for aliphatic, aromatic, terminal, and internal epoxides. Furthermore, exceptional TON and TOF were obtained exemplifying that this binary catalyst is ideal for sustainable large-scale cyclic carbonate preparation.

Data availability

The experimental details, structural characterization of 2 including X-ray diffraction studies (CCDC 2368776[†]), NMR, and a comparison table of COCs are provided in the ESI.[†]

Conflicts of interest

There are no conflicts to declare.

Acknowledgements

The authors thank SERB (financial support), Prof. Sri Sivakumar, and Dhyananand Yadav for the stirred tank autoclave reactor facility and IITK for infrastructure. Also, the authors, RC (IITK), SKS (CSIR, IITK), and IAB (UGC, IITK), thank the funding agencies for doctoral fellowships.

References

- (a) T. Yan, H. Liu, Z. X. Zeng and W. G. Pan, *J. CO₂ Util.*, 2023, **68**, 102355; (b) Q. W. Song, Z. H. Zhou and L. N. He, *Green Chem.*, 2017, **19**, 3707; (c) M. Aresta, A. Dibenedetto and A. Angelini, *Chem. Rev.*, 2014, **114**, 1709.
- Earth System Research Laboratories, Global Monitoring Laboratory, <https://gml.noaa.gov/ccgg/trends>, (July 2024).
- (a) Q. Liu, L. Wu, R. Jackstell and M. Beller, *Nat. Commun.*, 2015, **6**, 5933; (b) S. J. Poland and D. J. Darensbourg, *Green Chem.*, 2017, **19**, 4990; (c) P. P. Pescarmona, *Curr. Opin. Green Sustainable Chem.*, 2021, **29**, 100457; (d) C. A. L. Lidston, S. M. Severson, B. A. Abel and G. W. Coates, *ACS Catal.*, 2022, **12**, 11037; (e) V. Mishra and S. C. Perer, *Chem. Catal.*, 2024, **4**, 100796.
- B. Schöffner, F. Schöffner, S. P. Verevkin and A. Börner, *Chem. Rev.*, 2010, **110**, 4554.
- (a) C. C. Su, M. He, R. Amine, Z. Chen, R. Sahore, N. D. Rago and K. Amine, *Energy Storage Mater.*, 2019, **17**, 284; (b) C. Zhao, X. Luo, C. Chen and H. Wu, *Nanoscale*, 2016, **8**, 9511.
- Y. J. Zhang, J. H. Yang, S. H. Kim and M. J. Krische, *J. Am. Chem. Soc.*, 2010, **132**, 4562.
- P. P. Pescarmona and M. Taherimehr, *Catal. Sci. Technol.*, 2012, **2**, 2169.
- (a) A. A. Marciniak, K. J. Lamb, L. P. Ozorio, C. J. A. Mota and M. North, *Curr. Opin. Green Sustainable Chem.*, 2020, **26**, 100365; (b) S. K. Sachan and G. Anantharaman, *Inorg. Chem.*, 2021, **60**, 9238; (c) Y. Xiong, H. Wang, R. Wang, Y. Yan, B. Zheng and Y. Wang, *Chem. Commun.*, 2010, **46**, 3399.
- L. Guo, K. J. Lamb and M. North, *Green Chem.*, 2021, **23**, 77.
- B. H. Xu, J. Q. Wang, J. Sun, Y. Huang, J. P. Zhang, X. P. Zhang and S. J. Zhang, *Green Chem.*, 2015, **17**, 108.
- (a) C. Martín, G. Fiorani and A. W. Kleij, *ACS Catal.*, 2015, **5**, 1353; (b) A. Decortes, A. M. Castilla and A. W. Kleij, *Angew. Chem., Int. Ed.*, 2010, **49**, 9822.
- (a) D. F. Lopez, D. E. Salcedo, F. M. Nachtigall, L. S. Santos, M. A. Macias, R. S. Rojas and J. J. Hurtado, *Inorg. Chem.*, 2024, **63**, 9066; (b) X. Jiang, F. Gou, F. Chen and H. Jing, *Green Chem.*, 2016, **18**, 3567; (c) Z. A. K. Khattak, H. A. Younus, N. Ahmad, H. Ullah, S. Suleman, M. S. Hossain, M. Elkadi and F. Verpoort, *Chem. Commun.*, 2019, **55**, 8274; (d) H. Ullah, B. Mousavi, H. A. Younus, Z. A. K. Khattak, S. Chaemchuen, S. Suleman and F. Verpoort, *Commun. Chem.*, 2019, **2**, 42; (e) A. Sibouhi, P. Ryan, K. V. Axenov, M. R. Sundberg, M. Leskelä and T. Repo, *J. Mol. Catal. A: Chem.*, 2009, **312**, 87; (f) B. Wang, X. Cao, L. Wang, X. Meng, Y. Wang and W. Sun, *Inorg. Chem.*, 2024, **63**, 9156.
- (a) S. L. Dabb and N. C. Fletcher, *Dalton Trans.*, 2015, **44**, 4406; (b) A. Ehnborn, S. K. Ghosh, K. G. Lewis and J. A. Gladysz, *Chem. Soc. Rev.*, 2016, **45**, 6799.
- (a) P. Braunstein and F. Naud, *Angew. Chem., Int. Ed.*, 2001, **40**, 680; (b) A. Bader and E. Lindner, *Coord. Chem. Rev.*, 1991, **108**, 27.
- (a) S. S. Bera and M. Szostak, *ACS Catal.*, 2022, **12**, 3111; (b) A. A. Danopoulos, T. Simler and P. Braunstein, *Chem. Rev.*, 2019, **119**, 3730; (c) S. Hameury, P. de Fremont and P. Braunstein, *Chem. Soc. Rev.*, 2017, **46**, 632; (d) W. A. Herrmann, *Angew. Chem., Int. Ed.*, 2002, **41**, 1290; (e) E. Peris, *Chem. Rev.*, 2018, **118**, 9988.
- (a) I. A. Bhat, I. Avinash and G. Anantharaman, *Organometallics*, 2019, **38**, 1699; (b) I. A. Bhat, I. Avinash, S. K. Sachan, S. Singh and G. Anantharaman, *Eur. J. Inorg. Chem.*, 2021, **44**, 4560; (c) F. D. Monica, S. V. C. Vummaleti, A. Buonerba, A. D. Nisi, M. Monari, S. Milione, A. Grassi, L. Cavallo and C. Capacchione, *Adv. Synth. Catal.*, 2016, **358**, 3231.
- W. Y. Song, Q. Liu, Q. Bu, D. Wei, B. Dai and N. Liu, *Organometallics*, 2020, **39**, 3546.
- I. A. Bhat, *Late 3d Transition Metal Complexes Featuring a Multifunctional Heterobidentate NHC Ligand: Synthesis, Structure and Catalytic Applications*, Indian Institute of Technology (IIT) Kanpur, 2022.
- M. Siddique, M. Das and A. Rit, *Organometallics*, 2024, **43**, 1482.
- (a) W. M. Ren, Z. W. Liu, Y. Q. Wen, R. Zhang and X. B. Lu, *J. Am. Chem. Soc.*, 2009, **131**, 11509; (b) E. K. Noh, S. J. Na, S. Sujith, S. W. Kim and B. Y. Lee, *J. Am. Chem. Soc.*, 2007, **129**, 8082; (c) K. Nakano, T. Kamada and K. Nozaki, *Angew. Chem., Int. Ed.*, 2006, **45**, 7274; (d) H. Taube, *Chem. Rev.*, 1952, **50**, 69; (e) L. Suresh, J. Finnstad, K. W. Tornroos and E. L. Roux, *Inorg. Chim. Acta*, 2021, **521**, 120301.
- (a) L. P. da Silva, *J. Phys. Chem. C*, 2017, **121**, 16300; (b) X. Wang, L. Wang, Y. Zhao, K. Kodama and T. Hirose, *Tetrahedron*, 2017, **73**, 1190.